Superlattice Turing Structures in a Photosensitive Reaction-Diffusion System

Igal Berenstein, Lingfa Yang, Milos Dolnik, Anatol M. Zhabotinsky, and Irving R. Epstein
Department of Chemistry and Center for Complex Systems, MS 015, Brandeis University, Waltham, Massachusetts 02454-9110, USA
(Received 7 April 2003; published 29 July 2003)

Families of complex superlattice structures, consisting of combinations of basic hexagonal or square patterns, are found in a photosensitive reaction-diffusion system. The structures are induced by simple illumination patterns whose wavelengths are appropriately related to that of the system's intrinsic Turing pattern. Computer simulations agree with the structures and their stability. The technique offers a general approach to generating superlattices for use in information storage and other applications.

DOI: 10.1103/PhysRevLett.91.058302 PACS numbers: 82.40.Ck, 47.54.+r, 82.50.Hp

Superlattices are highly symmetric, sometimes strikingly intricate, structures composed of two or more simple component patterns (planforms), such as hexagons or squares, with appropriately related wavelengths. They are found in bacterial cell surface layers [1], have been proposed as a basis for the organization of cellular membranes [2], and, combined with supramolecular assembly, offer the prospect of improved functionality in miniature device construction [3]. They were originally studied in solid state physics [4] and are generated in two-frequency forced Faraday experiments [5]. Turing patterns, the stationary reaction-diffusion structures thought to play a role in morphogenesis [6,7], typically consist of a single fundamental hexagonal or striped planform, but a recent experiment [8] gave evidence for the "black eye" [9], a simple hexagonal superlattice Turing pattern, in the chlorine dioxide-iodine-malonic acid (CDIMA) reaction. We report here a method that generates families of increasingly complex hexagon- and square-based Turing superlattices in the CDIMA reaction. Simulations of a realistic model system [10] are in excellent agreement with both the structures and the stability of the observed superlattices.

The study of pattern formation in nonequilibrium reaction-diffusion systems began with the theoretical analysis of Turing structures. Until recently, however, few regular symmetric patterns have been found in experiment. Here we demonstrate that superlattices, which are symmetric patterns with long-range periodicity, can be induced within the parameter region where only labyrinthine Turing patterns, lacking symmetry and long-range order, arise spontaneously.

Details of the experimental procedure have been described previously [11]. In brief, a continuously-fed, unstirred, one-sided reactor with a 0.3 mm thick agarose gel layer as the working medium was fed with the reagents of the CDIMA reaction with initial concentrations $I_2 =$ 0.4 mM, malonic acid = 1.8 mM, $ClO_2 = 0.14$ mM, and polyvinyl alcohol (PVA) = 10 g/l. A striped labyrinthine pattern developed and became stationary within 10 h. Then, illumination for 5 min with uniform light ($70\ \mathrm{mW/cm^2}$ at the gel surface) from a quartz halogen lamp brought the system to a homogeneous steady state. After that, the intensity was changed to $23.6\ \mathrm{mW/cm^2}$, and a mask was placed between the light source and the reactor, with the image of the mask focused on the surface of the working area. We used masks with hexagonal and square patterns of circular spots with the transmittance of the masks determined by the sums of sinusoidal functions. We varied the ratio (R) of the spatial period of the illumination pattern to the average period of the original labyrinthine pattern in the range 0.8–6.0. Snapshots were taken under an intensity of $0.6\ \mathrm{mW/cm^2}$.

The illumination through the mask was maintained for 30 min, based on preliminary experiments, which showed that patterns under illumination became stationary within this time. After the illumination was turned off, some of the patterns evolved into superlattice Turing structures. Figure 1 shows superlattices induced with hexagonal masks with $R = 2$, 3, 4, and 5. The first superlattice, the black-eye pattern, consists of black spots inside white circles. Black corresponds to a high concentration of the triiodide-PVA complex. Other superlattices include honeycomb structures containing continuous black lines and persisted for more than 10 h before slowly beginning to deteriorate. All the superlattices preserved the positions and sizes of the unit cells of the original illumination patterns. When we used rational values of R, such as 2.4 or 3.2, we generated patterns similar to those obtained with the nearest integral R values, but these patterns gradually evolved into labyrinthine patterns. Superlattice patterns were also obtained using illumination through inverted hexagonal masks, where the center of each spot is opaque and the area between spots is transparent. Superlattice patterns formed with such masks resemble the superlattice patterns obtained with the corresponding original mask, though the latter patterns display fewer defects.

Figure 2 shows examples of superlattices induced with square masks with $R = 2.1$, 3.2, and 4.3, while with $R = 5.3$ a mixture of stripes and spots appeared and then evolved into a labyrinthine pattern. The square

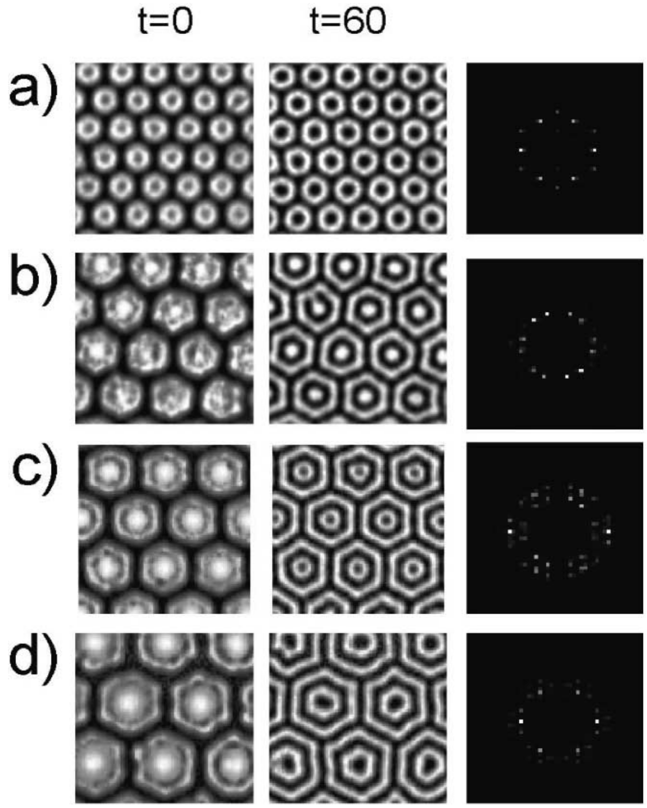

FIG. 1. Turing superlattices induced in the CDIMA reaction-diffusion system by illumination through a hexagonal pattern of transparent circles. The first column shows patterns at the end of illumination, the second column displays patterns 1 h later, and the third column contains Fourier spectra of the patterns in the second column. $R = $ (a) 2.0, (b) 3.0, (c) 4.0, (d) 5.0. The frame size is 5×5 mm.

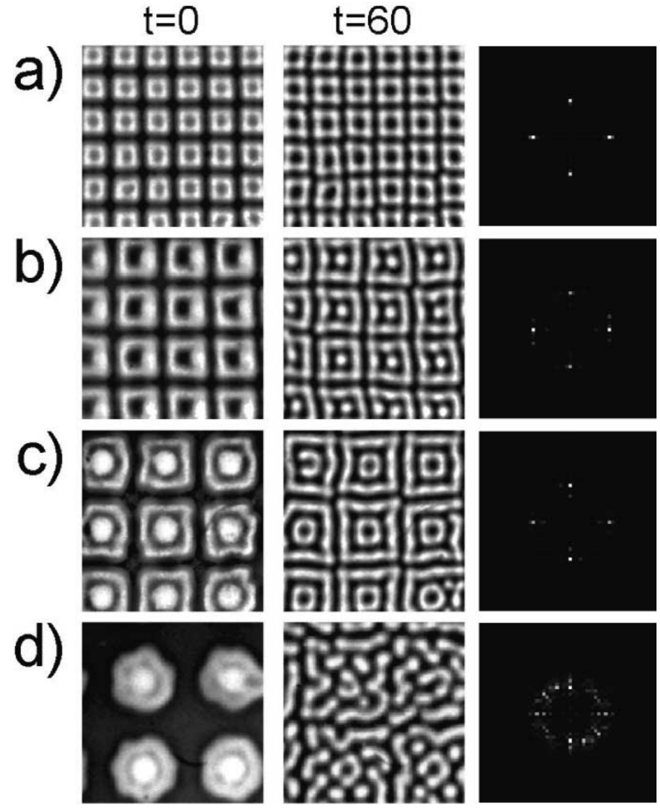

FIG. 2. Turing structures induced by illumination through square masks. Arrangement and size of the frames is the same as in Fig. 1. $R = $ (a) 2.1, (b) 3.2, (c) 4.3, (d) 5.3. $w_{\max} = $ (a) 0.02, (b)–(d) 0.06.

superlattices contained significant defects and deteriorated further during the next several hours, leading eventually to labyrinthine patterns. When R was an integer (e.g., 3.0 or 4.0) we obtained less symmetric patterns than those shown in Fig. 2.

Figure 3 shows patterns induced with hexagonal masks (w) in the modified Lengyel-Epstein (LE) model [10,12] given by the equations

$$u_t = a - u - 4uv/(1 + u^2) - w + \Delta u, \qquad (1)$$

$$v_t = \sigma\{b[u - uv/(1 + u^2)] + w + d\Delta u\}, \qquad (2)$$

where u and v are the dimensionless concentrations of $[I^-]$ and $[ClO_2{}^-]$, respectively; a, b, d, σ, and w are dimensionless parameters.

The simulation results are in good qualitative agreement with the experiment shown in Fig. 1. Masks with $R = 2.1$, 3.0, 4.0, and 5.0 induce superlattices, which remain stationary to the end of long runs (200–400 h of real time). A simple hexagonal lattice is formed by a resonant triplet of vectors: $\mathbf{k}_1 + \mathbf{k}_2 + \mathbf{k}_3 = 0$, with equal wave numbers [13]. Fourier spectra of superlattices show that the patterns contain several such triplets, which are shifted in phase and have wave numbers close to the average wave number of the labyrinthine pattern. Superlattices can be induced for a range of spatial periods of the illumination pattern; i.e., R can deviate significantly from an integer. The resulting superlattice preserves the period of the mask. A superlattice induced with R near an integer N displays concentration oscillations along the principal translation axes in which one spatial period contains N maxima. We designate such a pattern superlattice-N.

Most importantly, our simulations suggest that the superlattice patterns are stable. To confirm the stability, established superlattices were subjected to global perturbation by small amplitude natural labyrinthine patterns for times of the order of the time for development of the superlattice. The perturbed patterns relaxed back to the original superlattices. We also studied competition between labyrinthine patterns and superlattices. We subjected part of a rectangular area to illumination, while the remaining part was kept "dark." Figure 4 shows a limited invasion of the labyrinthine pattern into the superlattice region during the transition period after switching off the illumination. This invasion results in

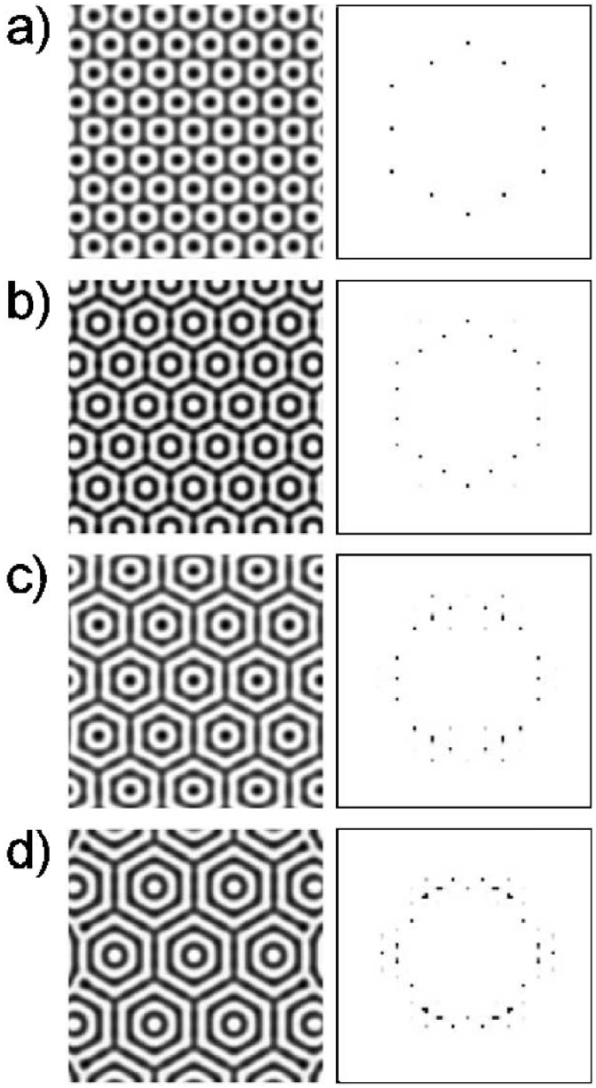

FIG. 3. Stable hexagonal superlattice Turing structures in the modified LE model. The first column displays the stationary patterns; the second column shows their Fourier spectra. $R =$ (a) 2.1, (b) 3.0, (c) 4.0, (d) 5.0. In our simulations $a = 12$, $b = 0.2$, $d = 1$, and $\sigma = 50$. The frame size is 128×128 space units (s.u.).

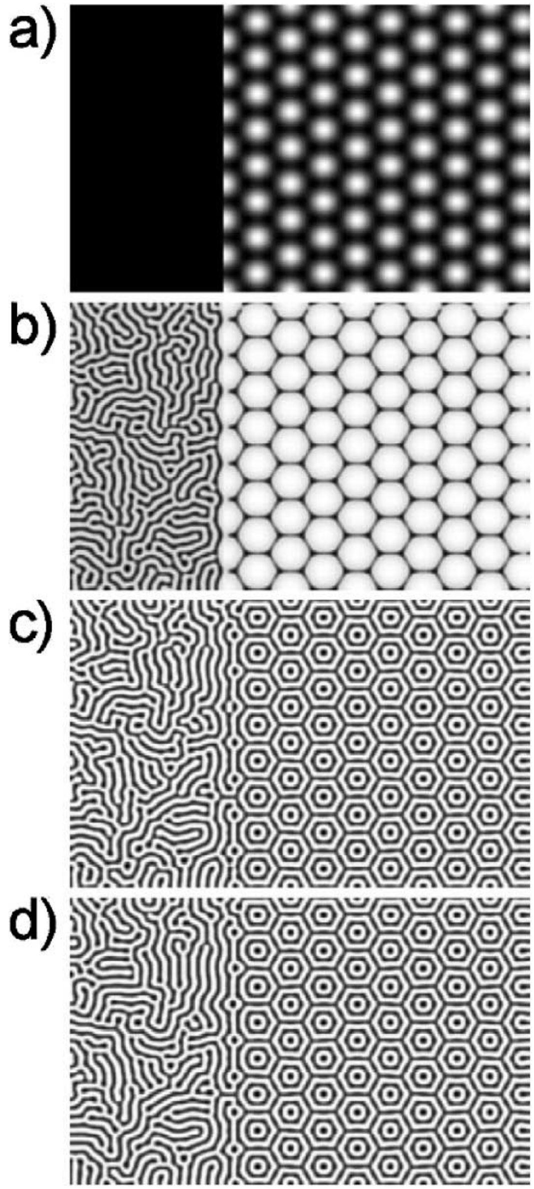

FIG. 4. Coexistence of a superlattice Turing structure and a labyrinthine pattern in the model. (a) The illumination pattern, under which the superlattice structure and a labyrinthine pattern develop simultaneously from random initial conditions. (b) The patterns immediately after the illumination is switched off. (c) The superlattice has developed together with the boundary that separates it from the labyrinthine pattern. (d) After a long time, the labyrinthine pattern has evolved slightly, but there is no change in the superlattice or the boundary. $R = 4$; frame size is 384×256 s.u.; time = (a) 0, (b) 80, (c) 200, (d) 1000 time units.

formation of a narrow stripe-dot boundary between the two regions parallel to the original boundary [Fig. 4(c)]. After that, some rearrangement takes place in the labyrinthine portion of the system, but no further changes occur in the superlattice pattern [Fig. 4(d)]. In the simulations, all hexagonal superlattices-N ($2 \leq N \leq 5$) and square superlattice-3 are stable. There was no significant difference between simulations with zero flux and periodic boundary conditions.

Previous studies have shown that near the boundaries of the Turing domain simple hexagons are stable [13], but deeper inside this domain, hexagonal patterns become unstable to stripelike perturbations and are converted to stripe patterns. Still deeper within the Turing domain, stripe patterns undergo the Eckhaus instability, resulting in labyrinthine patterns. The basic square pattern is generally unstable [13]. We were able to induce superlattice structures in the central region of the Turing domain, where the spectrum of Turing instability is quite wide and the basic symmetric patterns are unstable. In our experiments, several superlattices persisted for long times but ultimately deteriorated into labyrinthine patterns. Since the corresponding patterns in the model are stable, we suggest that instability in the experiments arises from imperfections in the experimental system. We are currently working to determine which deviations of the experiment from the model may be sources of instability.

Superlattice patterns have been observed previously in nonequilibrium reaction-diffusion [8,10], hydrodynamic [5], magnetohydrodynamic [14], and optical [15] systems. In most cases, they are generated by external time-periodic forcing. In autonomous systems, they emerge spontaneously, due to a relevant instability. Here we have shown that superlattices can be generated by a brief, spatially periodic, forcing in a system where they cannot emerge spontaneously and that the patterns thus induced are stable in computer simulations. This approach should be applicable to the generation of superlattice patterns in other physical and physicochemical systems such as nonlinear optical systems, where they can, in principle, be used for information storage.

This work was supported by the National Science Foundation under Grant No. CHE-9988463.

[1] D. Pum and U. B. Sleytr, Trends Biotechnol. **17**, 8 (1999).
[2] P. Somerharju, J. A. Virtanen, and K. H. Cheng, Biochim. Biophys. Acta **1440**, 32 (1999).
[3] T. Yokoyama, S. Yokoyama, T. Kamikado, Y. Okuno, and S. Mashiko, Nature (London) **413**, 619 (2001).
[4] D.L. Smith and C. Mailhiot, Rev. Mod. Phys. **62**, 173 (1990); P.V. Braun, P. Osenar, and S. I. Stupp, Nature (London) **380**, 325 (1996).
[5] H. Arbell and J. Fineberg, Phys. Rev. Lett. **81**, 4384 (1998); Phys. Rev. E **65**, 036224 (2002); J. L. Rogers, M. F. Schatz, O. Brausch, and W. Pesch, Phys. Rev. Lett. **85**, 4281 (2000).
[6] A. M. Turing, Philos. Trans. R. Soc. London B **237**, 37 (1952).
[7] H. Meinhardt, *Models of Biological Pattern Formation* (Academic, London, 1982).
[8] C. Zhou, H. Guo, and Q. Ouyang, Phys. Rev. E **65**, 036118 (2002).
[9] G. H. Gunaratne, Q. Ouyang, and H. L. Swinney, Phys. Rev. E **50**, 2802 (1994).
[10] I. Lengyel and I. R. Epstein, Science **251**, 650 (1991).
[11] M. Dolnik, I. Berenstein, A. M. Zhabotinsky, and I. R. Epstein, Phys. Rev. Lett. **87**, 238301 (2001); I. Berenstein, M. Dolnik, A. M. Zhabotinsky, and I. R. Epstein, J. Phys. Chem. A **107**, 4428 (2003).
[12] A. K. Horvath, M. Dolnik, A. P. Muñuzuri, A. M. Zhabotinsky, and I. R. Epstein, Phys. Rev. Lett. **83**, 2950 (1999).
[13] *Chemical Waves and Patterns*, edited by R. Kapral and K. Showalter (Kluwer, Dordrecht, 1995).
[14] H. J. Pi, S. Y. Park, J. Lee, K. J. Lee, Phys. Rev. Lett. **84**, 5316 (2000).
[15] M. A. Vorontsov and B. A. Samson, Phys. Rev. A **57**, 3040 (1998).